

KALKER'S COEFFICIENT c_{11} AND ITS INFLUENCE ON THE DAMPING AND THE RETUNING OF A MECHANICAL DRIVE TORSION SYSTEM OF A RAILWAY VEHICLE

VOJTĚCH DYBALA

Czech Technical University in Prague, Faculty of Mechanical Engineering, Department of Automotive, Combustion Engines and Railway Engineering, Technická 4, 160 00 Prague 6, Czech Republic

correspondence: vojtech.dybala@fs.cvut.cz

ABSTRACT. Within the research of electromagnetically excited torsion oscillations in the mechanical part of traction drive systems of modern railway vehicles, which has been realized at the Faculty of mechanical engineering at the CTU in Prague, there are two separate simulation models in use. The basic calculation model, which is utilized to gain basic characteristics of the torsion system as natural frequencies and natural modes of oscillations. And the complex simulation model, which simulates a drive of the vehicle. This contribution is focused on the basic calculation model, which has been built in MATLAB. This model in its first version did not apply the contact between wheels and rails. It was necessary to find out, if this simplification is relevant with respect to subsequent simulations within the complex simulation model and its results. Therefore, the contact interaction as a traction force in longitudinal direction in the wheel-rail contact was realized via the Kalker's linear theory. This article deals with the comparison between models with and without the implementation of the wheel-rail contact and its influence on the damping within the torsion system and retuning of the torsion system.

KEYWORDS: Kalker, natural frequency, railway vehicle, torsion system, wheel-rail contact.

1. INTRODUCTION

One of the typical features of modern electrical railway vehicles is the individual mechanical drive of the wheel-set, e.g. see Figure 1. In principal it means that each wheel-set has its own propelling unit. This unit mostly consists of an electrical traction motor, a gearbox and a coupling connecting both of them. For sure there are more concepts of such a mechanical drive unit.

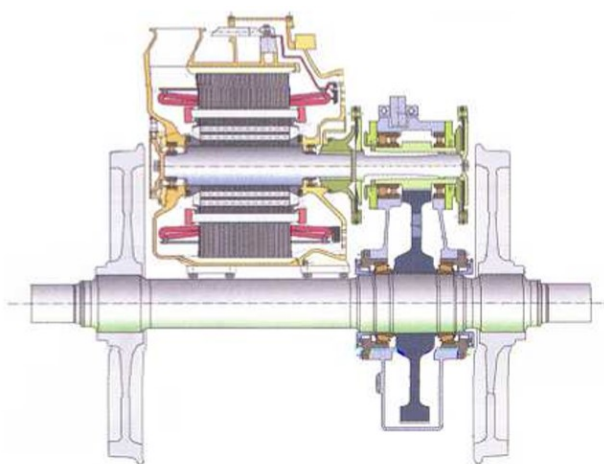


FIGURE 1. A partly-suspended drive of a locomotive [1].

For purposes of this research a fully-suspended drive layout has been applied. This type of an individual drive consists of an electrical traction motor, a gearbox and a hollow shaft, which transmits driving and braking power between the gearbox and the wheel-set

– Figure 2. Because generally this research is focused on high-speed and high-power railway vehicles, the fully-suspended type of a drive train was chosen, as it is a typical and an appropriate layout for this type of vehicles.

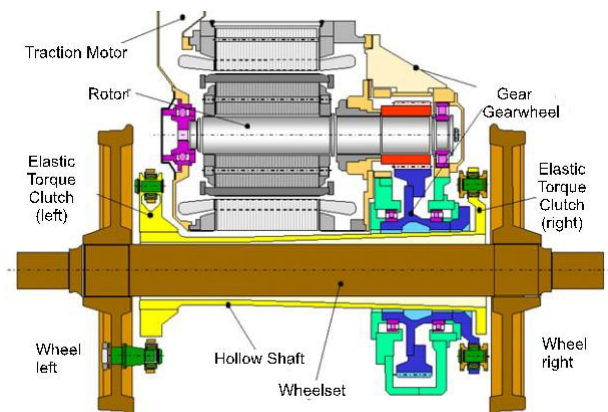


FIGURE 2. A fully-suspended drive of a locomotive [2].

2. BASIC MATHEMATICAL MODEL

This mathematical model, built in MATLAB, is utilized to provide basic characteristics of a torsion system, which schematically represents the design of a mechanical drive train of a railway vehicle.

The basic characteristics are:

- natural frequencies of oscillations
- natural modes of oscillations

Knowledge of these characteristics is supposed to be important for evaluation of frequency analysis, which will be carried out in subsequent simulations in the above-mentioned complex simulation model, built in MATLAB Simulink. Now the complex simulation model applies some simplifications to do simulations effective in terms of simulation time, amount of data and goals of the research. The basic calculation model supposes also some simplifications as the interaction in the wheel-rail contact. Because of the frequency analysis it is appropriate to do a review if the simplification of the basic calculation model is reasonable and if there can be a significant impact on the evaluation frequency analysis.

2.1. MODEL WITH NO WHEEL-RAIL CONTACT

The mathematical model is based on the scheme of the torsion system (Figure 3), which respects the layout of the fully-suspended drive presented in Figure 2.

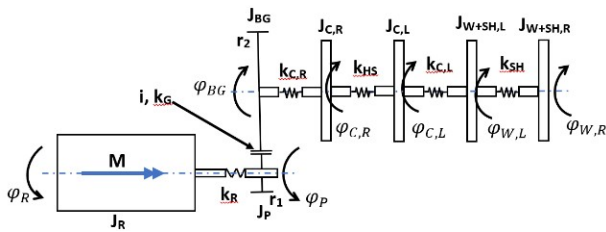


FIGURE 3. Torsion system scheme – fully-suspended drive [3].

Equations of motion describing this system were derived via the Lagrange method. The matrix notation of these equation of motion is (1). To calculate natural modes and natural frequencies of oscillations these equations are solved as a system without the vector of excitation $[M]$, see (2).

$$[J][\ddot{\varphi}] + [k][\varphi] = [M] \quad (1)$$

$$[J][\ddot{\varphi}] + [k][\varphi] = [0] \quad (2)$$

The system (2) was solved via the function $eig(k, J)$, which is a pre-programmed function in MATLAB. This function returns:

- an *eigen* vector representing rotation angle $\varphi_{i,j}$ for a rotation mass J_i and j natural mode of oscillation
- an *eigen* values vector $[\lambda_j]$ representing j natural angle frequency $\Omega_j = \sqrt{\lambda_j}$

The *eigen* values are transformed into natural frequencies f_j via the formula (3).

$$f_j = \frac{\sqrt{\lambda_j}}{2\pi} \quad (3)$$

2.2. MODEL WITH A WHEEL-RAIL CONTACT

The wheel-rail contact was implemented into the calculation model via longitudinal traction forces T_1 , which can be seen in the top view of the drive train – Figure 4. The wheel-rail contact is simplified so, that

lateral forces and spin moment between the wheel and the rail are neglected. Practically it means that it represents rolling of a cylindrical wheel on rails, not conical profile wheels and sinus movements of the wheel-set is neglected. Also forces T_1 on both sides are supposed to be same.

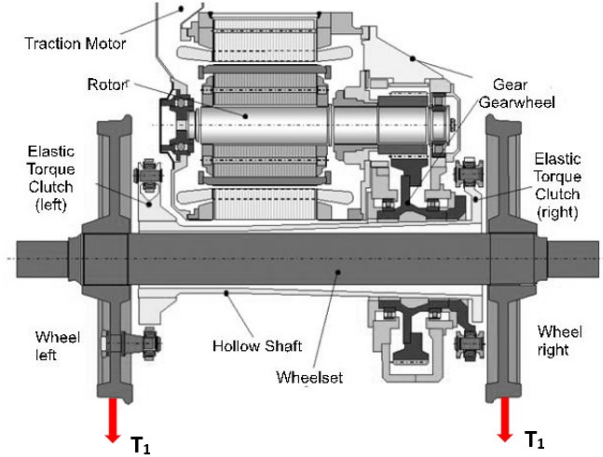


FIGURE 4. Visualization of wheel-rail forces – top view.

The longitudinal traction force T_1 is calculated via Kalker's linear theory for the wheel-rail contact (4).

$$T_1 = c_{11} a_{el} b_{el} G s_x = C_1 s_x = k_1 s_x \quad (4)$$

In this article details about the Kalker's theory will not be presented, but they can be found in [4–6]. For purposes of this contribution the value of Kalker's coefficient $c_{11} = 4,984$ is taken as a fact. That coefficient itself can varies. Because that theory is linear, its validity is limited for small values of slip with respect to adhesion characteristic – phase I in Figure 5. For the area of higher slip (phase II) the direction of the curve k_1^* decreases.

While the value of c_{11} can be supposed for good conditions in the wheel-rail contact (dry rails), for worst conditions (wet or dirty rails) it can decrease as well. This fact is presented in Figure 6 within Popovici's adhesion characteristics.

And therefore because of both effects, the calculations were carried out also for variations of c_{11} , specifically for $c_{11}/2$ and $c_{11}/4$.

$$s_x = \frac{r_k \omega_k - v_x}{v} \quad (5)$$

Due to above mentioned simplifications also only the wheel slip s_x in the longitudinal direction is supposed. Its deduction is presented in Figure 7 and its mathematical representation is formula (5).

$$[J][\ddot{\varphi}] + [b][\dot{\varphi}] + [k][\varphi] = [0] \quad (6)$$

Within the torsion system scheme (Figure 8) and subsequently the equations of motion in the matrix representation (6) the force T_1 creates a damping element in the wheel-rail contact. This damping defines

3. CALCULATION RESULTS

Results of calculations in sections 3.1 and 3.2 below are respective to the theory from sections 2.1 and 2.2 and the subsequent conclusion aims to make an analysis of the velocity influence on the retuning of the torsion system via damping.

3.1. MODEL WITH NO WHEEL-RAIL CONTACT

The torsion system scheme, which respects the design of the fully-suspended drive in Figure 2 is a system with 7 degrees of freedom and seven natural frequencies of oscillation were calculated, see Table 1. Because the torsion system in this state was considered as a free system the first natural frequency is 0Hz and it matches with a free rotation of the system. Natural modes of oscillation complying with the natural frequencies are presented in Figure 10 to Figure 16. Such a considered state of the torsion system can be agreed with the situation when a railway vehicle does not generate any force in the wheel-rail contact – standstill of the vehicle or drive without traction or brake force.

Natural frequencies of torsion system [Hz]						
1.	2.	3.	4.	5.	6.	7.
0	6	57	337	572	857	2403

TABLE 1. Natural frequencies overview [3].

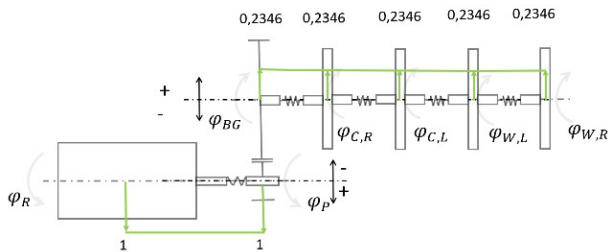


FIGURE 10. First natural mode of torsion oscillations [3].

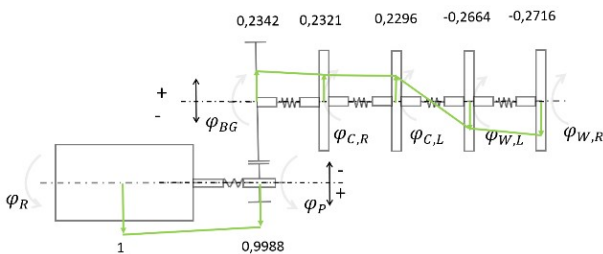


FIGURE 11. Second natural mode of torsion oscillations [3].

Table 2 provides a description of these natural modes with respect to dominant oscillation of a specific rotation mass.

Order of natural modes	Respective natural frequency [Hz]	Dominant oscillations of a mass	Less significant oscillations
1.	0	Own free rotation	–
2.	6	Wheel-set towards hollow shaft	–
3.	57	Wheels of wheel-set	–
4.	337	Wheel-set towards hollow shaft	Pinion towards rotor
5.	572	Pinion towards rotor	–
6.	857	Hollow shaft joints	Wheel-set towards hollow shaft Gear wheel towards hollow shaft
7.	2403	Pinion towards rotor Pinion towards gear wheel	–

TABLE 2. Description of natural modes [3].

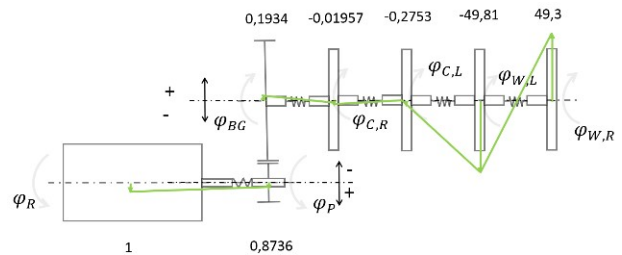


FIGURE 12. Third natural mode of torsion oscillations [3].

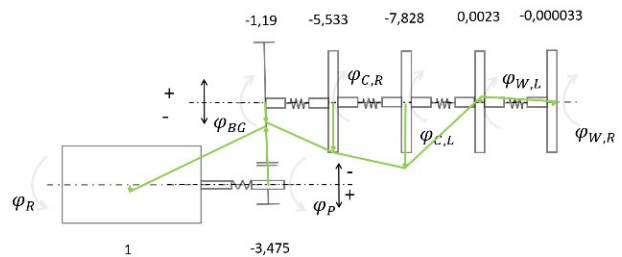


FIGURE 13. Fourth natural mode of torsion oscillations [3].

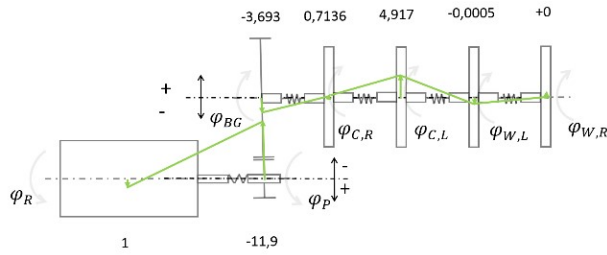


FIGURE 14. Fifth natural mode of torsion oscillations [3].

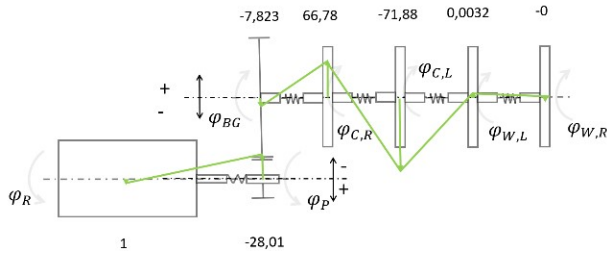


FIGURE 15. Sixth natural mode of torsion oscillations [3].

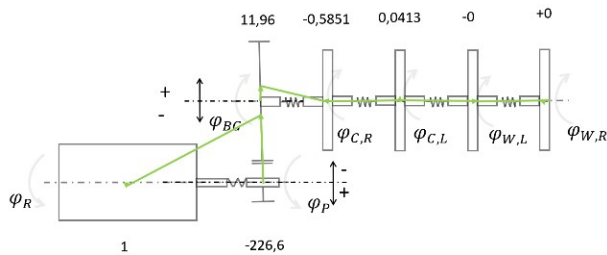


FIGURE 16. Seventh natural mode of torsion oscillations [3].

3.2. MODEL WITH A WHEEL-RAIL CONTACT

In this section the attention will be put on calculated eigenvalues and respective natural frequencies.

The first group of calculations was done for the value of the Kalker's coefficient $c_{11} = C_1$. With respect to the damping Figure 17 shows that, the damping reaches very high values in low velocities and strongly decrease with increasing velocity. This fact can be concluded with respect to the third eigenvalue, which relates to torsion oscillations of the wheel-set, see Table 2. Regarding natural frequencies see Figure 18. A small change in the value of the second one can be observed, from 6Hz to 4Hz. A significant change can be observed regarding the third one when its value decreased from 57Hz to 0Hz. This means that the damping in the wheel-rail contact is so high, that it suppresses torsion oscillations of the wheel-set.

For the second group of calculations, where $C_1 = c_{11}/2 = k_1*$, see Figure 5 and Figure 6, the situation changed. The damping (Figure 19) was very high in low velocities again and suppressed oscillations of the wheel-set on the frequency of 57Hz. With increasing velocity, the damping decreases. Between 100 km/h and 105 km/h retuning of the system appeared. There

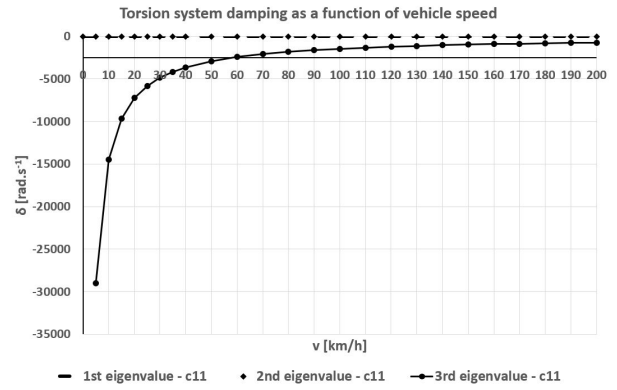


FIGURE 17. Damping as a function of velocity – c_{11} .

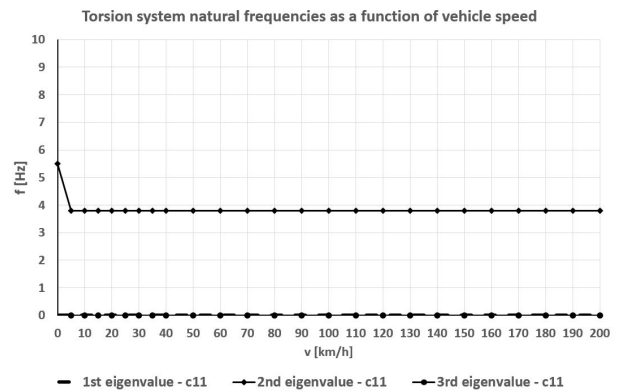


FIGURE 18. Natural frequencies as a function of velocity – c_{11} .

is a visible jump in damping and change in the third natural frequency (Figure 20), which started to grow. Then the third natural frequency increases with decreasing damping and approximate to the value of 57 Hz. Also, a small change in the value of the second natural frequency from 6Hz to 4Hz was observed.

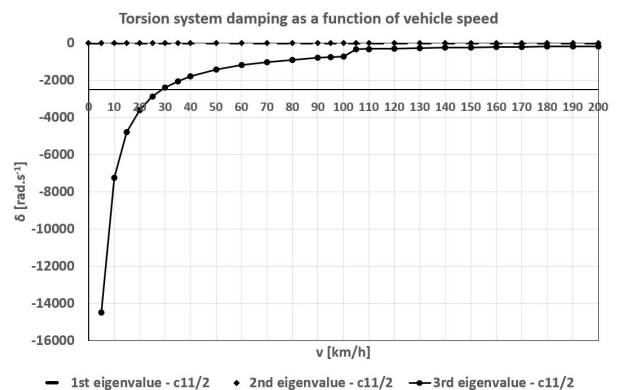


FIGURE 19. Damping as a function of velocity – $c_{11}/2$.

In the third group of calculations, where $C_1 = c_{11}/4 = k_1*$, see Figure 5 and Figure 6, the results were equivalent to results from the second group. The difference, which Figure 21 and Figure 22 presents, is that the point of torsion system retuning occurs in lower velocity, between 50 km/h and 55 km/h. A small

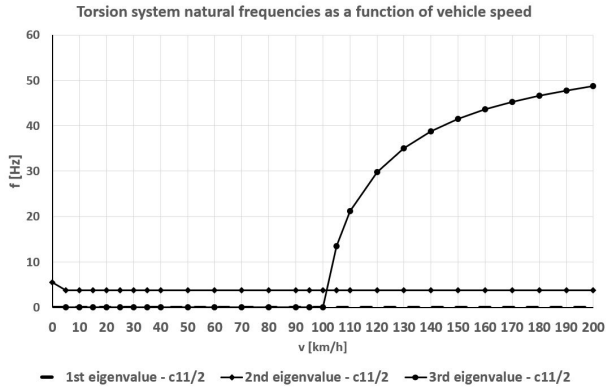


FIGURE 20. Natural frequencies as a function of velocity – $c_{11}/2$.

change in the value of the second natural frequency from 6Hz to 4Hz was observed again.

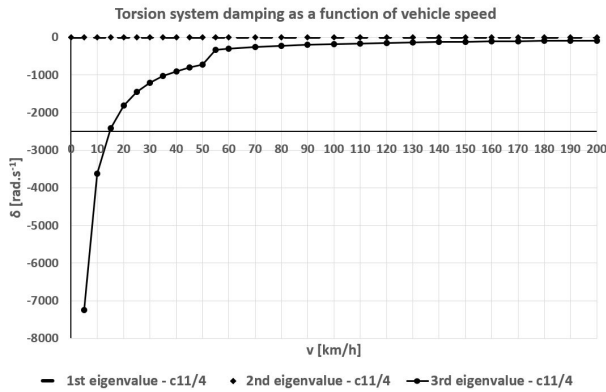


FIGURE 21. Damping as a function of velocity – $c_{11}/4$.

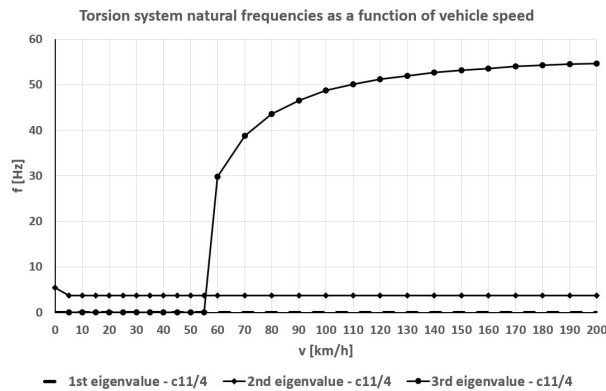


FIGURE 22. Natural frequencies as a function of velocity – $c_{11}/4$.

The fourth, the fifth, the sixth and the seventh eigen value and respective damping parameters and natural frequencies are not mentioned, because the calculations did not show any influence of the variation of values of the velocity and the Kalker’s coefficient.

4. CONCLUSIONS

Results of calculations presented in Figure 17 to Figure 22 proved, that the wheel-rail contact can signifi-

cantly influence a behavior of a torsion system, which means to change some natural frequencies. Specifically, the third natural frequency related to the oscillations of the wheel-set itself in a very strong way and weakly the second natural frequency related to oscillations of the wheel-set towards the hollow shaft. On the other hand, it was presented, that the variability of parameters, which characterize the wheel-rail contact, don’t influence the rest of the torsion system. With respect to a research it can practically mean, that for a research oriented on a wheel-set torsion oscillations and related problematics, the effect of the wheel-rail contact should be considered. On the other hand, within a research of torsion phenomenon regarding the rest of a torsion system, as traction motor, gears and coupling, the wheel-rail contact can be neglected.

LIST OF SYMBOLS

- a_{el} main half-axis of contact ellipse [m]
- b_{el} secondary half-axis of contact ellipse [m]
- b, b_{W-R} damping parameter [Nms.rad⁻¹]
- c_{11} Kalker’s coefficient [-]
- f natural frequency [Hz]
- f_{dmp} natural frequency of damped system [Hz]
- J mass of rotation [kg.m²]
- k torsion stiffness [Nm.rad⁻¹]
- M external torque [Nm]
- T_1 Tangential force [N]
- r_k Wheel radius [m]
- s_x Wheel slip [%]
- φ angle rotation [rad]
- $\dot{\varphi}$ time derivative of angle rotation [rad.s⁻¹]
- $\ddot{\varphi}$ second time derivative of angle rotation [rad.s⁻²]
- λ eigenvalue [-]
- Ω natural angle frequency [rad.s⁻¹]
- Ω_{dmp} natural angle frequency of damped system [rad.s⁻¹]
- ω_k angular speed of a wheel [rad/s]
- δ oscillation damping [rad/s]

ACKNOWLEDGEMENTS

This research has been realized using the support of The Technology Agency of the Czech Republic, programme National Competence Centres, project #TN01000026 Josef Bozek National Center of Competence for Surface Transport Vehicles This support is gratefully acknowledged.

REFERENCES

- [1] T. Fridrichovský. *Studie disertační práce*. Praha, 2017.
- [2] V. Dybala, M. Libenský, B. Šulc, C. Oswald. *Slip and Adhesion in a Railway Wheelset Simulink Model Proposed for Detection Driving Conditions Via Neural Networks*. In SBORNÍK vědeckých prací Vysoké školy báňské – Technické univerzity Ostrava, Řada strojní, Ostrava, 2018.
- [3] V. Dybala. *The Electromagnetically Excited Resonance of the Pinion in Fully-Suspended Drive of a Locomotive and its Sensitivity on the Torsion Stiffness of the Rotor Shaft*. In Sborník abstraktů konference STČ, Praha, 2021.

- [4] J. Kolář. *Teoretické základy konstrukce kolejových vozidel*. Praha: Česká technika – nakladatelství ČVUT, 2009, p. 276.
- [5] J. Kolář. *Zborník prednášok II. – XX. Medzinárodná konferencia – Súčasný problémy v kolajových vozidlách*. In *Dynamika individuálneho pohonu dojkolí s nápravovou prevodovkou*, Žilina, 2011.
- [6] J. Kolář. *Problémy modelování vlivu svislých nerovností trati do dynamiky pohonu dvojkolí*. In *Železničná doprava a logistika XI*, pp. 38–47, 2015.
- [7] R. Popovici. *Friction in Wheel-Rail Contacts*. Enschede, The Netherlands: University of Twente, 2010.